Journal of Materials and Environmental Sciences
ISSN : 2028-2508
CODEN : JMESCN

J. Mater. Environ. Sci., 2019, Volume 10, Issue 7, Page 668-676

http://www.jmaterenvironsci.com

Electrochemical Analysis of Evans Blue by Surfactant Modified Carbon Nanotube Paste Electrode

B. M. Amrutha [1,2], J. G. Manjunatha [1*], S. Aarti Bhatt [2], N. Hareesha [1]

[1] *Department of Chemistry, FMKMC College, Madikeri, Constituent College of Mangalore University, Karnataka, India*
[2] *Department of Chemistry, NMAM Institute of Technology, Nitte, Karnataka, India*

Received 03 July 2019,
Revised 08 Aug 2019,
Accepted 08 Aug 2019

Keywords
- ✓ Cyclic Voltammetry,
- ✓ Carbon nanotube,
- ✓ TX-100,
- ✓ Evans blue,
- ✓ Tartrazine.

manju1853@gmail.com

Tel: +91-08272228334

Abstract

Electrochemical sensor for the specific and sensitive detection of Evans blue (EB) at physiological pH in 0.2M phosphate buffer solution (PBS) was developed by the surface modification using Triton X -100 (TX-100) surfactant. The cyclic voltammetry (CV) studies show enhanced peak separation, appreciable sensitivity, selectivity and stability which allowed this TX-100 surfactant modified carbon nanotube paste electrode (TX-100MCNTPE) to analyse EB individually and simultaneously along with tartrazine (TZ) in the potential range of 0.2 V to 0.7 V. The electrode morphology was characterised by field emission scanning electron microscopy (FESEM). The oxidation potential of EB shifted negatively, and enhanced irreversible oxidation peak current was observed at 0.505V which served as the analytical response. In the prime condition, the anodic peak current of EB increased linearly, and two linear ranges were observed from 10 µM to 100 µM with the limit of detection (LOD**)** of 5.06 µM and limit of quantification (LOQ) of 16.87 µM. Scan rate studies reveal that the entire process in the electrode surface is adsorption controlled. The modified electrode showed excellent reproducibility, repeatability and antifouling properties

1. Introduction

Going back to the 20th century a large number of blue dyes like methylene blue, patent blue, trypan blue, evans blue and many more were synthesized. Out of these EB, an azo dye with the molecular formula $C_{34}H_{24}N_6Na_4O_{14}S_4$ is the one which is habitually used tracer as a biological dye and clinical diagnostic agent [1]. It is thoroughly water soluble and also sturdily binds with serum albumin [2-5]. EB is extensively used in biomedicine for the assessment of blood volume, recognition of lymph nodes and location of the tumour due to its water solubility and gradual excretion. The extensive range of neurological disorder caused by intrinsic mechanism of blood brain barrier encouraged a renewed awareness to study their function. Complete analysis of such disorders requires markers to know the functional changes at the barrier between the brain, barrier and cerebrospinal fluid. EB is the extensively used marker for brain barrier experiment. The advantage of EB compared with other dyes is that a very small concentration is sufficient [6]. The sense organs of the animal will get stained if it is injected in excess [7,8]. If EB is activated with green light, it emits a splendid red fluorescence [9]. This property of EB dye can be used in the characterisation of lymph nodes that void the liver [10]. Series of EB derivatives are labelled with PET isotopes and are used to acquire diagnostic images and deliver a therapeutic dose of radiation to the patient due to their refined half-life in the blood. EB does not affect the healthy cell, but it invades and persist within the damaged cells. EB is also used for the screening of abnormalities in the developing foetus. Continuous and regular exposure to EB is considered to be a hazardous irritant and potential carcinogen. It causes respiratory tract irritation like wheezing, coughing and shortness of breath [11]. Hence it is necessary to develop a basic and swift method for the detection of the dyes not only for analytical studies but also for diagnostic research. The electroanalytical technique turns out to be the effective tool since it is simple, cost-effective, facile surface

renewing and it is a quick way of analysing clinical diagnostic agents like EB persisting in the blood and urine samples. Structure of EB is depicted in Figure 1.

CNTs are hollow carbon structures with a diameter in nanoscale. Their length is more compared to the diameter, and it is composed of one or more concentric tubules [12]. Due to their distinctive mechanical, electronic and chemical properties CNT's have received significant consideration in the field of electrochemical sensing. Their exceptional miniatured structure, substantial specific surface area, alterable sidewall, soaring conductivity make CNT's as platform to conjugate other compounds at their surface. CNTs are more reliable in CV studies because of their competence to provide low LOD, antifouling property, high sensitivity and diminished overpotential. CNTs are likely to have consistent active sites which enhances their electrocatalytic activity in comparison with other carbon paste electrodes [13-16]. By modifying the CNT's with suitable surfactant their stability and responsiveness can be enhanced. Surfactant modified electrodes have superior electroanalytical properties like a wide potential window, low detection limit exceptional sensitivity and antifouling properties in the surface [17,18].

Surfactants are surface active agents with an amphiphilic character which has the potential to change the behaviour at the electrode and solution interface by enhancing the electrochemical responses [19]. Adsorption of surfactant on the surface of the electrode aggregates the electron allocation, moderately boosts the peak current, alter the redox potential or charge transfer coefficients, along with varying the steadiness of electrogenerated intermediates and electrochemical products [20]. The choice of modifiers depends on their ability to reduce over potential for the reduction and oxidation of electro active species in contrast with the electrode which is unmodified. Surfactant modifiers like CTAB, SDS, TX-100, poly(glycine), nanoparticles are used which are found to be enormously sensitive to acid and basic media [21]. In the present work we are employing TX-100 as surface modifier because of its extensive application in amending the carbon surface. TX-100 is a non-ionic surfactant with a unique molecular structure that has a hydrophilic polyethylene oxide chain and an aromatic hydrophobic group. It has the capacity to orient itself at the interface of the solution and the electrode surface which will have significant impact on the electrochemical processes like peak current, charge transfer coefficient and they can also amend the stability of electrogenerated species [22,23]. TX-100MCNTPE gives enhanced peak current compared to BCNTPE.

CV techniques are considered to be the efficient tool for investigating the electrochemical behaviour of analyte since it offers both qualitative and quantitative information. This article reports the effective oxidation of EB with a highly sensitive and stable CV response at TX-100MCNTPE. The outcome proves that the modified electrode exhibits a well-defined oxidation peak without any interferences.

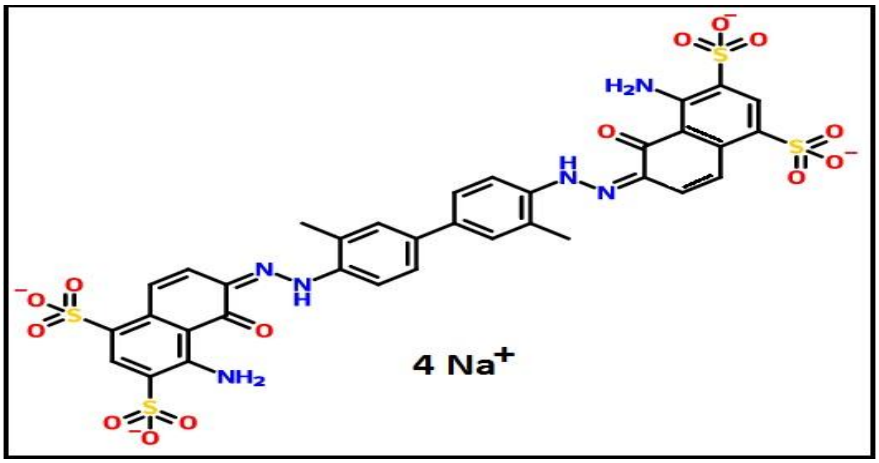

Figure 1: Structure of EB

2. Material and Methods

2.1.Apparatus

Electrochemical experiments was performed by using the model CHI-6038E [CH- Instrument from USA] combined with a conventional three-electrode cell. The three-electrode cell consists of a calomel electrode

employed as reference electrode, a platinum wire which acts as a counter electrode and a TX-100MCNTPE and bare carbon nanotube paste electrode (BCNTPE) as working electrode. Field emission scanning electron microscopy for surface morphology study was done by the instrument operating at 5.00 kV (DST-PURSE Laboratory, Mangalore University).

2.2. Reagents and Chemicals

Multi-walled carbon nanotube with a dimension of 30-50 nm and length of 10-30 µm was procured from Sisco research laboratories, Maharashtra, India. Evans Blue was purchased from Himedia Laboratories Pvt. Ltd. Mumbai, India. Silicone oil, Monosodium phosphate, Disodium phosphate, Tartrazine and TX-100 surfactant were obtained from Nice chemicals, Cochin, India. 25×10^{-4} M solution of TX-100 was prepared in distilled water. EB (1×10^{-4} M) and TZ (1×10^{-4} M) stock solutions were prepared by dissolving it in double distilled water. PBS solution of strength 0.2 M was prepared by mixing the required quantity of 0.2 M NaH_2PO_4 and 0.2 M Na_2HPO_4.

2.3. Preparation of BCNTPE and TX-100MCNTPE

After optimising the ratio of CNT powder to the binder, the carbon nanotube paste electrode (CNTPE) was prepared by mixing the CNT powder and silicon oil in the ratio of 60:40 (w/w) in the agate mortar using a pestle to get a homogeneous mixture. A part of the resulting homogeneous paste was packed into the cave of a teflon tube of diameter 3mm. To get a smooth surface of the BCNTPE, the surface is rubbed on the smooth weighing paper. A copper wire inserted into the teflon tube establishes contact with the external circuit. In the present work immobilisation was carried out by using 10µl of surfactant and allowed to stand for five minutes, since at this optimisation point, it was observed that the highest peak current value with good resolution was obtained due to critical aggregate concentration. 10 µl of surfactant TX-100 was dropped onto the surface of BCNTPE by a micro injector and left for 5 minutes so that maximum adsorption of the surfactant on the electrode surface takes place after which the excess was washed off with double distilled water.

3. Results and discussion

3.1. Surface Characterisation

Morphological study of electrode surface was characterised by FESEM. Figure 2a and 2b illustrate the FESEM images of BCNTPE and TX-100 MCNTPE respectively. The FESEM image of BCNTPE (Figure 2a) portrays irregular morphology at the electrode surface. But FESEM images of TX-100MCNTPE (Figure. 2b) shows agglomerated morphology, specifying the modification of the electrode surface.

(a) (b)

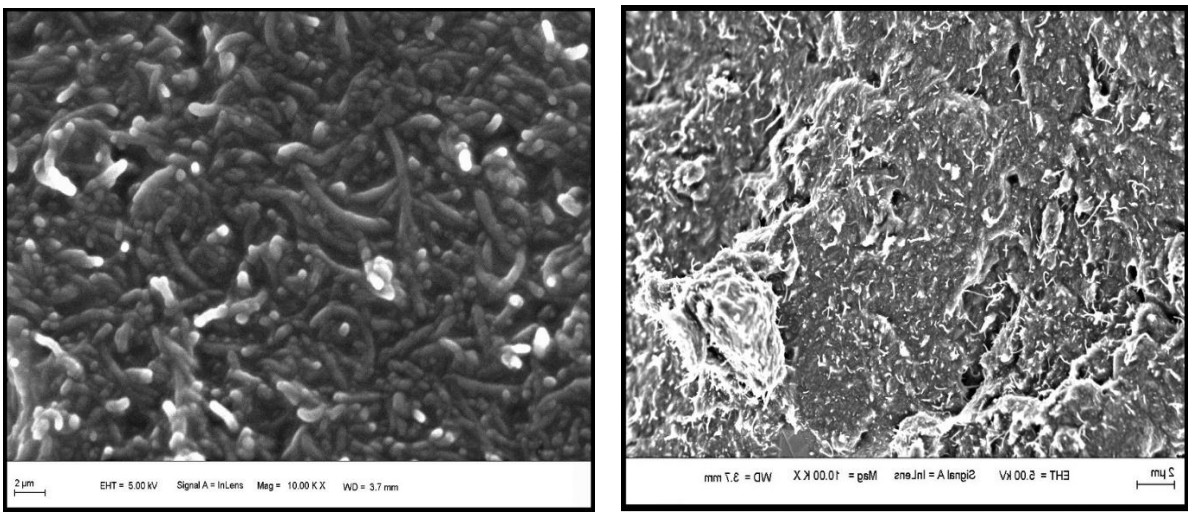

Figure 2: (a) Surface morphology of BCNTPE, (b) TX-100MCNTPE

The surface of TX-100MCNTPE shows spongy like appearance with cavities and pores in presenting a high ratio of surface area. The surfactant is adsorbed on the BCNTPE surface forming a distinct molecular layer which is reliant on the dissolution of a hydrophobic chain of the surfactant in silicon oil and, the hydrophilic chain is exposed to the electrolyte. This produces plenty of active sites resulting in enhanced current.

3.2. Influence of pH

The pH of a solution will have a robust impact on the electrochemical behaviour of the analyte. Sharper response escorted with higher sensitivity can be obtained by optimising the pH of the solution. PBS of 0.2 M as supporting electrolyte over a pH range of 6.0-8.0 was considered for the electrochemical investigation of EB at a scan rate of 0.1 V/s (Figure. 3a). Hence with the increase of pH the peak potential shifted to the less positive side because of the hindrance of oxidation at lower proton concentration [24,25]. Anodic peak current increases from pH 6 to 7 and a gradual decrease in anodic peak current at later pH was observed. The magnitude of the current is reliant on the rate of the electrochemical reaction. Hence from the plot of I_{pa} vs. pH (Figure. 3b), it is apparent that highest current response with enhanced sensitivity and reliable shape of voltammogram was observed at neutral pH 7 due to faster electron transfer, and hence pH 7 is considered for subsequent determinations. Linear relationship was observed for plot (Figure. 3c) E_{pa} vs pH with a linear regression equation E_{pa} (V) = 0.8876 + 0.0534 pH and R = 0.9696. The slope of 0.053 V/pH is in close approximation to the theoretical value of 0.059 V/pH specifies that the number of protons and electrons involved in the oxidation of EB in the proportion of 1:1 [26-28].

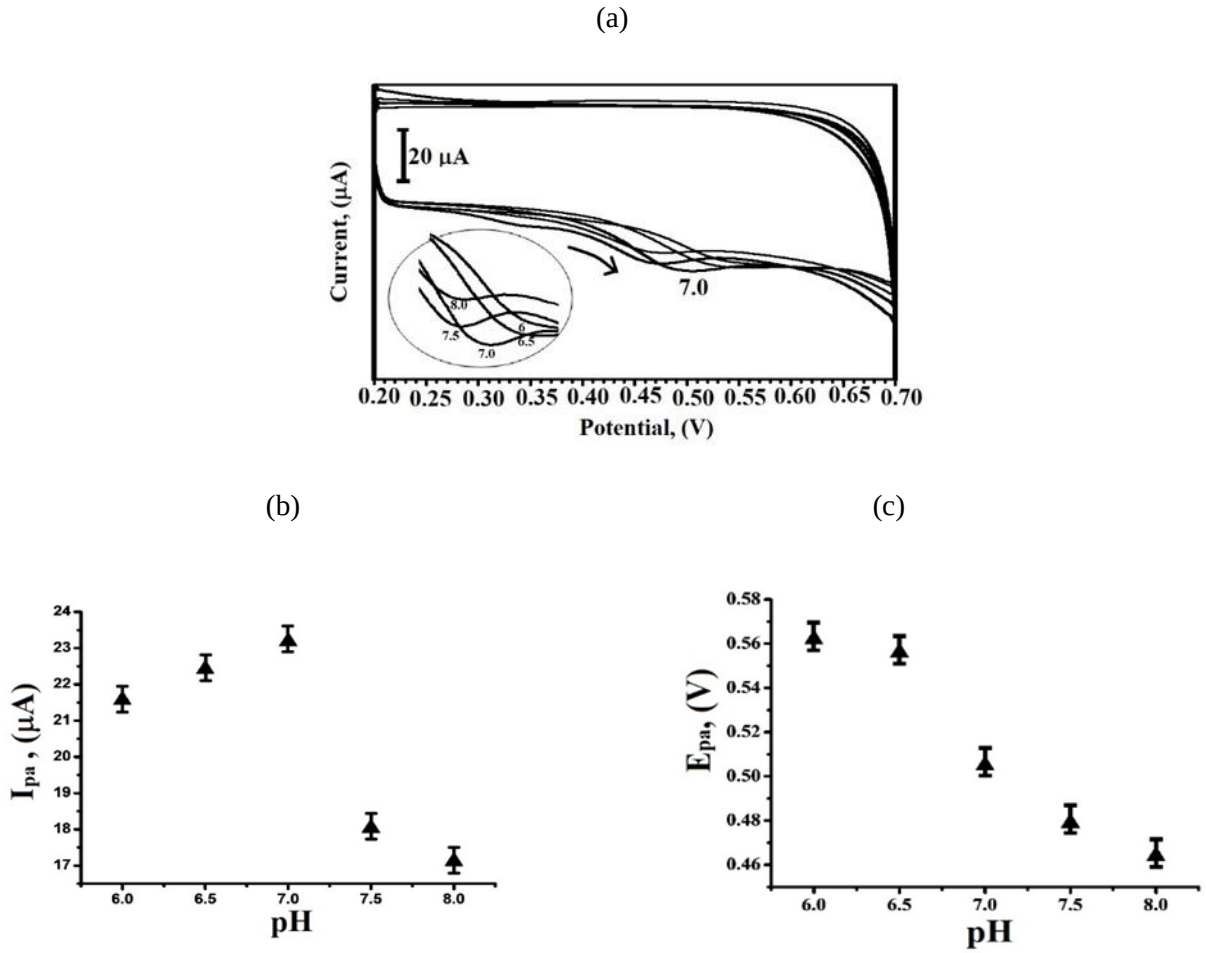

Figure 3: (a) Cyclic voltammogram (v = 0.1V/s) of EB (1×10^{-4} M) in 0.2 M PBS of pH 7.0 at TX-100MCNTPE at several pH values ranging from 6.0 to 8.0, (b) plot of anodic peak current (I_{pa}) vs pH (c) plot of anodic peak potential (E_{pa}) vs. pH.

3.3. Voltammetry response of EB

The captivating properties of TX-100 MCNTPE in enhancing the electrochemical behaviour of EB under different conditions can be illuminated by using CV at BCNTPE and TX-100MCNTPE. Figure. 4a represents the cyclic

voltammograms of 1×10^{-4} M EB at BCNTPE and TX-100MCNTPE in the optimum conditions. Curve a shows poor sensitivity due to the low rate of electron transfer. But the voltammogram obtained for TX-100 MCNTPE (curve b) in the identical condition gives a peak with high current signal of 23.19 µA due to fast rate of electron transfer. The presence of oxidation peak for TX-100MCNTPE manifests the modification of BCNTPE by a thin film of TX-100 which remarkably enhances the reactivity of modified electrode towards the oxidation of EB. Since the reverse scan shows no reduction peak, it is therefore clear that the electrochemical reaction was an irreversible process. The CV depicted in Figure. 4b elucidate that the anodic peak current and anodic peak potential responses were not disclosed in the absence of EB (curve a) but under the identical condition, in the presence of EB (curve b), an improved voltammetry response is obtained.

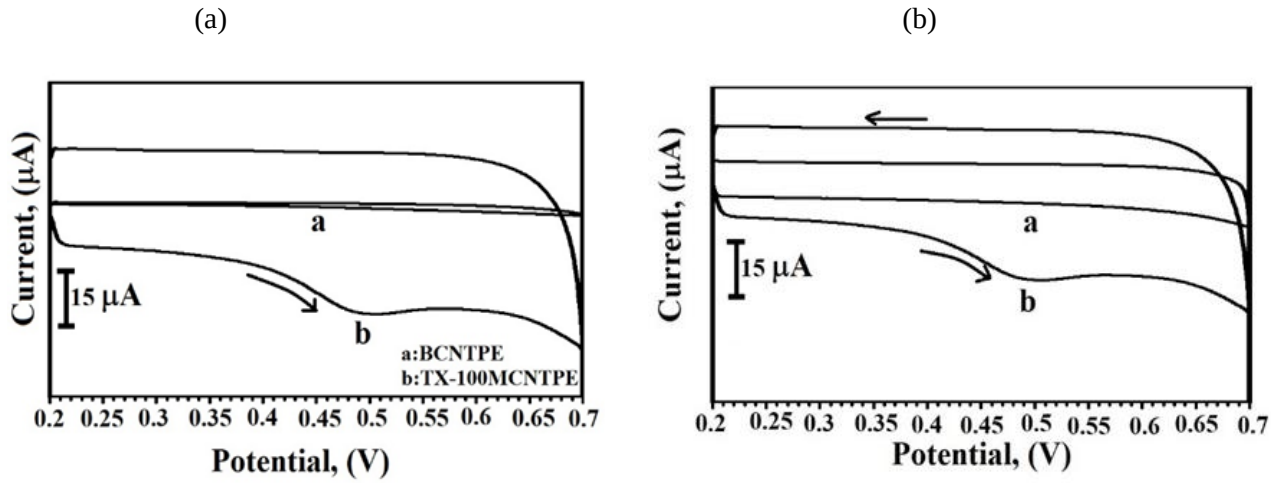

Figure 4: (a) Cyclic Voltammogram of 1×10^{-4} M EB in 0.2 M PBS buffer of pH 7 at BCNTPE (curve a) and TX-100MCNTPE (curve b) at a scan rate of 0.1 V/s. (b) Cyclic Voltammogram without EB in 0.2 M PBS buffer of pH 7 at TX-100MCNTPE (Curve a) and with 1×10^{-4} M EB in 0.2 M PBS (curve b) at a scan rate of 0.1 V/s.

3.4. Impact of scan rate on peak current of EB

The relation between anodic peak current and scan rate provides information about the electrochemical mechanism. Hence the electrochemical behaviour of EB at various scan rates from 0.1 V/s to 0.250 V/s in optimum condition was analysed by cyclic voltammetry studies. Figure. 5a clarifies the fact that with the increase of scan rate anodic peak current also increases.

Plot of anodic peak current (I_{pa}) v/s scan rate (v) (Figure. 5b) portrays descent linear relationship with a linear regression equation I_{pa}(µA) = 1.7696 + 0.1883 v (V/s) and R= 0.9969. This demonstrates that at pH 7 the electrode process was adsorption controlled rather than diffusion controlled. Further, there was a linear relationship between log I_{pa} and log *v* (Figure. 5c) corresponding to the following equation log I_{pa} (µA) = 2.2401 + 0.9298 log *v* (V/s); R=0.9937. Slope of 0.9298 is in the close ballpark with the ideal value for adsorption- controlled process. The plot of E_{pa} and log *v* (Figure. 5d) explain the linear relationship between the anodic peak potential and scan rate and can be described by the following equation E_{pa} (V)= 0.5788 + 0.0947 log *v* (V/s) with R= 0.9659.

According to Laviron's equation, considering the plot of E_{pa} vs log *v* for a totally irreversible adsorption-controlled electrode process, can be defined by the equation,

$$E_{pa} = Eo + \left(\frac{2.303RT}{\propto nF}\right) log \left(\frac{RTK^{\circ}}{\propto nF}\right) + \left(\frac{2.303RT}{\propto nF}\right) \log v$$

above equation n represents the number of electrons transferred, α is the charge transfer coefficient which is considered to be 0.5 for irreversible electrode process, k^o the standard rate constant of the reaction, F is Faraday constant, E_o the formal potential. Other symbols have their usual significance. Slope is considered to be equal to 2.303RT/αnF. By substituting the respective values, the numerical value obtained for n is 1.2 and is considered as 1. Hence the oxidation reaction of EB at TX-100MCNTPE proceeds through one electron transfer [29-31].

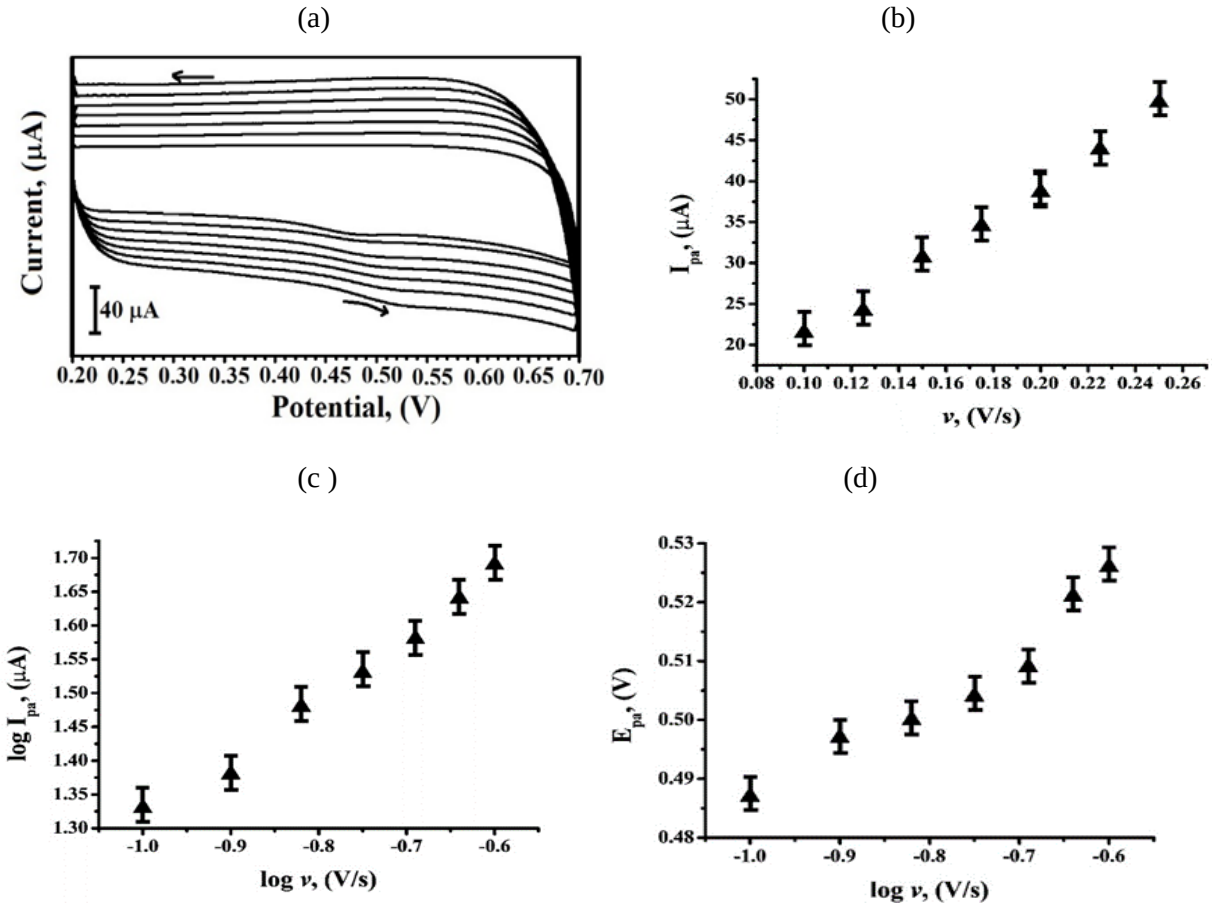

Figure 5: (a) Cyclic Voltammogram of EB (1×10^{-4} M) in 0.2 M PBS at diverse scan rates from 0.1 V/s to 0.250 V/s. (b) Plot of Ipa v/s scan rate, (c) Plot of log I_{pa} v/s log *v* (d) Plot of Epa v/s log v.

3.5. Calibration plot and influence of concentration of EB on the peak current

The concentration of EB was varied from 2μM to 200 μM, and according to the electrochemical response observed from Figure 6, it's clear that anodic peak current values augmented linearly with the increase of EB under optimum conditions.

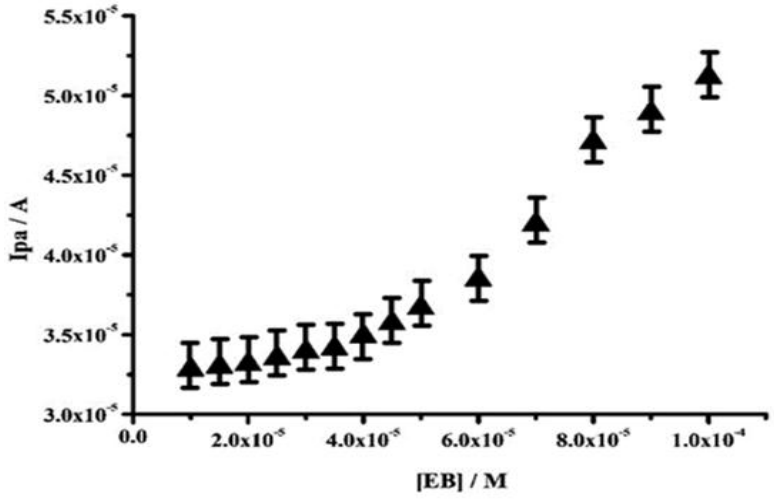

Figure 6: Calibration plot for the determination of EB at TX-100MCNTPE in 0.2 M PBS of pH 7.

The plot shows two linear ranges from 10 μM to 100 μM, that is from 10 μM to 50 μM and from 60 μM to 100 μM. The first linear range is considered which has an R value of 0.9916. LOD and limit of quantification LOQ were evaluated by equations LOD = 3S/N and LOQ = 10S/N (N represents the slope of calibration curve and S represents the standard deviation of the peak currents of the blank solution) [32, 33]. The LOD and LOQ values were found to be 5.06 μM and 16.87 μM respectively.

3.6. Simultaneous detection of EB and TZ using TX-100MCNTPE

Tartrazine is used as an edible dye in soft drinks, packaged food, cosmetics which goes into the human body. So, the core intention of this work is to detect EB and TZ simultaneously using TX-100MCNTPE in optimum condition and is depicted in Figure. 7. Peak with less current sensitivity is exhibited by BCNTPE for both the EB and TZ (curve a). This indicates that the BCNTPE failed to portray enhanced voltammetry signal for the simultaneous determination of EB and TZ. The fouling effect of the electrode surface with the oxidized products of EB and TZ is assumed to be the reason for poor sensitivity [34,35]. But, two oxidation peaks corresponding to EB at 0.533 V and TZ at 0.885 V were observed in CV when TX-100MCNTPE was used (curve b). Hence the obtained result proves that EB exhibits good resolution with well-separated peaks in the presence of edible dyes like TZ. The difference between the oxidation peak potentials of EB and TZ was 0.35 V.

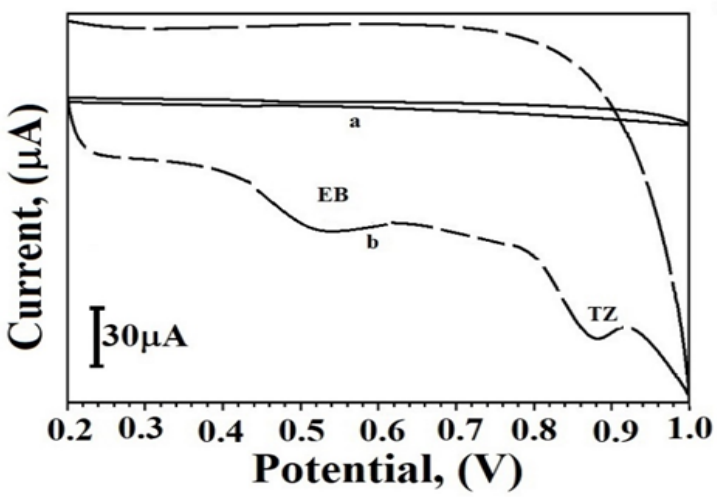

Figure 7: Simultaneous determination of 1 × 10^{-4} M EB and 1 × 10^{-4} M TZ in 0.2 M PBS of pH 7 by TX-100MCNTPE (a) and BCNTPE (b).

3.7. Examination of Repeatability, Reproducibility and Stability

The sensing performance of the modified electrode under the ideal condition can be gauged by parameters like repeatability, reproducibility and stability. Well characterised reproducible and repeatable peaks were observed in the recorded CV which proves the fact that the electrode has the capability for the generation of a stable, reproducible surface. TX-100MCNTPE reveals healthy reproducibility and repeatability with RSD values comprised of 3.76% (n=4) and 3.03% (n=3) respectively. The stability of the modified electrode was appraised by running 28 consecutive cycles. Percentage degradation was calculated [36]:

Percentage degradation =I_{pn}/I_{p1} ×100 which shows that 96% of the initial current was retained.

Conclusion

The projected TX-100MCNTPE was successfully utilised for the electrocatalytic oxidation of EB in 0.2 M PBS (pH = 7) at a scan rate of 0.1 V/s. The modified sensor showed a refined resolution towards the electrocatalytic action for the oxidation of EB, which displays magnification of the anodic peak current due to the elevated precise surface area, fine electronic properties and robust adsorptive nature. The LOD and LOQ were found to be 5.06 µM and 16.87 µM respectively. The oxidation reaction of EB at TX-100MCNTPE is found to proceed through one electron transfer. The working sensor can be used for the simultaneous determination of EB along with the existence of TZ by CV. The modified sensor exhibits good linearity, repeatability and reproducibility.

References

1. H.M. Evans and W. Schulemann, The action of vital stains belonging to the benzidine group, *Jstor*, 39 (1914) 443–54. doi:10.1126/science.39.1004.443
2. Y. Linpeng, X. Xing, Y. Peipei, N. Yicheng and C. Feng, Review Article Evans Blue Dye : A Revisit of its Applications in Biomedicine, *Contrast Media & Mol Imaging*, (2018) 1-11. doi.org/10.1155/2018/7628037

3. M. Wolman, I. Klatzo, E. Chui et al, Evaluation of the dyeprotein tracers in pathophysiology of the blood-brain barrier, *Acta Neuropathol*, 54 (1981) 55–61.
4. A. Saria, J. M. Lundberg, Evans blue fluorescence: quantitative and morphological evaluation of vascular permeability in animal tissues, *J. Neurosci Methods*, 8 (1983) 41-49. doi.org/10.1016/0165-0270(83)90050-X
5. L. F. Yen, V. C. Wei, E. Y. Kuo and T. W. Lai, Distinct Patterns of Cerebral Extravasation by Evans Blue and Sodium Fluorescein in Rats, *Plosone*, 8 (2013) 685-95. doi.org/10.1371/journal.pone.0068595
6. N. R. Saunders, K. M. Dziegielewska, K. Mollgard and M. D. Habgood, Markers for blood-brain barrier integrity: how appropriate is Evans blue in the twenty-first century and what are the alternatives?, *Front. Neurosci*., 29 (2015) doi.org/10.3389/fnins.2015.00385.
7. A. Manaenko, H. Chen, J. Kammer, J.H. Zhang, and J. Tang, Comparison Evans Blue injection routes : Intravenous versus intraperitoneal, for measurement of blood-brain barrier in a micehemorrhagemodel, *J Neurosci Methods*, 195 (2011) 206-10. doi : 10.1016/j.jneumeth.2010.12.013
8. B. T. Roller, J.M. Munson, B. Brahma, P. J. Santangelo, S.B. Pai and R.V. Bellamkonda, Evans blue nanocarriers visually demarcate margins of invasive gliomas, *Drug Deliv Transl Re*, 5 (2015) 116–124. doi:10.1007/s13346-013-0139-x
9. O. Steinwall and I. Klatzo, Selective vulnerability of the blood-brain barrier in chemically induced lesions, *J Neuropathol Exp Neurol*, 25 (1966) 542–59. doi:10.1097/00005072-196610000-00004
10. M. Zheng, J. Yu and Z. Tian, Characterization of the liver draining lymph nodes in mice and their role in mounting regional immunity to HBV, *Cell Mol Immunol*, 10 (2013) 143–50. doi:10.1038/cmi.2012.59
11. B. N. Ramesh, A. M. Mahalakshmi, S. Mallappa, Vascular permeability and Evans blue dye : a physiological and pharmacological approach, *JAPS*, 4 (2014) 106-13. doi: 10.7324/JAPS.2014.41119 ISSN 2231-3354
11. M. T. Carmen and C. M. May, Carbon nanotube biosensors, *Front Chem*, 3 (2015) 3-59. doi: 10.3389/fchem.2015.00059
12. H. Chengguo and H. Shengshui, Review Article Carbon Nanotube-Based Electrochemical Sensors : Principles and Applications in Biomedical Systems, *J Sensors*, (2009) 1-40. doi.org/10.1155/2009/187615
13. C. Raril and J. G. Manjunatha, Carbon Nanotube Paste Electrode for the Determination of Some Neurotransmitters: A Cyclic Voltammetric Study, *Mod Chem Appl*, 6 (2018). doi:10.4172/2329-6798.1000263
14. C.M. Tilmaciu, M.C. Morris, Carbon nanotube biosensors, *Front Chem*, 3 (2015) 59. doi:10.3389/fchem.2015.00059
15. Kurusu F, Tsunoda H, Saito A, Tomita A, Kadota A, Kayahara N, Karube I, Gotoh M. The advantage of using carbon nanotubes compared with edge plane pyrolytic graphite as an electrode material for oxidase-based biosensors, *Analyst*, 12 (2006) 1292-98. doi:10.1039/b608904f
16. F. ValentiniAziz, A. Silvia, O. M. Letizia, T. G. Palleschi, Carbon Nanotube Purification, Preparation and Characterization of Carbon Nanotube Paste Electrodes, *Anal. Chem*, 9(2003) 5413-5421. doi.org/10.1021/ac0300237
17. W. Joseph and M. Mustafa, Carbon nanotube/teflon composite electrochemical sensors and biosensors, *J Anal Chem*, 75 (2003) 2075–79. doi:10.1021/ac030007
18. H. Beitollahi and S. Iran, Electrochemical behaviour of Carbon nanotube/ Mn (III) salen doped carbon paste electrode and its application for sensitive determination of N-acetylcysteine in the presence of folic Acid, *Int. J. Electrochem. Sc*, 7 (2012) 7684 – 98.
19. M. Kanit, M. Siriboon, The Fabrication of in Situ Triton X-100 on Multi-Walled Carbon Nanotubes Modified Gold Electrode for Sensitive Determination of Caffeine, *Int. J. Electrochem. Sci*, 13 (2018) 58 – 70. doi:10.20964/2018.01.39
20. J. G. Manjunatha, B. E. Kumara Swamy, G. P. Mamatha, G. Ongera, M.T. Shreenivas and B. S. Sherigara, Electrocatalytic Response of Dopamine at Mannitol and Triton X-100 Modified Carbon Paste Electrode : A Cyclic Voltammetric Study, *Int. J. Electrochem. Sci*, 4 (2009) 1706 – 18.
21. T. Girish, J. G. Manjunatha, C. Raril and N. Hareesha, Determination of Riboflavin at Carbon Nanotube Paste Electrodes Modified with an Anionic Surfactant, Chemistry Select, 4 (2019) 2168-73. doi:10.1002/slct.201803191

22. G. K. Jayaprakash, B. E. K Swamy, N. Casillas, R. Flores-Moreno, Analytical Fukui and cyclic voltammetric studies on ferrocene modified carbon electrodes and effect of Triton X-100 by immobilization method, *Electrochimica Acta*, 258 (2017) 1025-1034. Xxx.
23. J.G. Manjuntha, G. K. Jayaprakash, Electrooxidation and Determination of Estriol Using a Surfactant Modified Nanotube Paste Electrode, *Eurasian J Anal Chem*, 14 (2019) 225-231. doi.org/10.29333/ejac/20190101
24. A. G. Alarcon, A. S. Corona, P. M. Palomar, H. A. Rojas, R. M. Romero et al, Selective electrochemical determination of dopamine in the presence of ascorbic acid using sodium dodecyl sulfate micelles as masking agent, *Electrochim. Acta*, 53 (2008) 3013-20. doi.org/10.1016/j.electacta.2007.11.016.
25. A. S. Corona, A. G. Alarcon, R. M. Romero, A. Cuan, M. T. Ramirez-Silva, M. L. Hernandez et.al, Influence of CTAB on the electrochemical behavior of dopamine and on its analytic determination in the presence of ascorbic acid, J. Appl Electroche, 40 (2010) 463-74. doi:10.1007/s10800-009-0017-x
26. P. S. Nagaraj, J.M. Shweta, T.N. Sharanappa, Electrochemical behavior of an antiviral drug acyclovir at fullerene-C60-modified glassy carbon electrode, *Bioelectrochemistry*, 88 (2012) 76-83. doi.org/10.1016/j.bioelechem.2012.06.004
27. C. Raril and J. G. Manjunatha, Carbon Nanotube Paste Electrode for the Determination of Some Neurotransmitters : A Cyclic Voltammetric Study Modern Chemistry & Applications, *Mod Chem Appl*, 6 (2018) 2-8. doi:10.4172/2329-6798.1000263
28. N. B. Minh Phuong, A.L. Cheng, S. Gi Hun, Electrochemical detection of dopamine with polyglutamic acid patterned carbon nanotube electrodes, *Biochip J*, 6 (2012) 149-156. doi:10.1007/s13206-012-6207-3
29. N. Hareesha, J.G. Manjunatha, C. Raril and T. Girish, Design of novel Surfactant Modified Carbon Nanotube Paste Electrochemical Sensor for the Sensitive Investigation of Tyrosine as a Pharmaceutical Drug, *Adv Pharm Bull*, 9 (2019) 1-6. doi:10.1039/C2AY25528F
30. N. Spataru, B. V. Sarada, E. Popa, D. A. Tryk and A. Fujishima, Voltammetric Determination of L-Cysteine at Conductive Diamond Electrodes, *Anal. Chem*, 73 (2001) 514–519. doi.org/10.1021/ac000220v
31. N. Hareesha, J.G. Manjunatha, C. Raril and T. Girish, Sensitive and Selective Electrochemical Resolution of Tyrosine with Ascorbic Acid through the Development of Electropolymerized Alizarin Sodium Sulfonate Modified Carbon Nanotube Paste Electrodes, *Chemistry Select*, 4 (2019) 4559–67. doi:10.1002/slct.2019007
32. N. H. Rajesh, P. S. Nagaraj, S. T. Nandibewoor, Electro-oxidation and determination of trazodone at multi-walled carbon nanotube-modified glassy carbon electrode, *Talanta*, 79 (2009) 361-68. doi.org/10.1016/j.talanta.2009.03.064.
33. C. Raril, J.G. Manjunatha, Voltammetric determination of anthrone using cetyl trimethyl ammonium bromide surfactant modified carbon paste electrode, *Biomed. J. Sci. & Tech. Res.*, 11 (2018) 1-5. doi:10.26717/BJSTR.2018.11.002108
34. M. M Charithra, J. G. Manjunatha, Poly (l-Proline) modified carbon paste electrode as the voltammetric sensor for the detection of Estriol and its simultaneous determination with Folic and Ascorbic acid, Materials Science for Energy Technologies, 2 (2019) 365-71. doi.org/10.1016/j.mset.2019.05.002
35. J. G. Manjunatha, M. Deraman, N. H. Basria, A. Talib, Fabrication of poly (Solid Red A) modified carbon nano tube paste electrode and its application for simultaneous determination of epinephrine, uric acid and ascorbic acid, *Arab J Chem*, 11 (2018) 149-158. doi.org/10.1016/j.arabjc.2014.10.00
36. N. Prinith, J. G. Manjunatha, Surfactant modified electrochemical sensor for determination of Anthrone - A cyclic voltammetry, *Materials Science for Energy Technologies*, 3 (2019) 408-16. doi:10.1016/j.mset.2019.05.004